

## Role of Brownian motion hydrodynamics on nanofluid thermal conductivity

William Evans

Lockheed Martin Corporation, Niskayuna, New York 12301 and Mechanical Engineering Department, Rensselaer Polytechnic Institute, Troy, New York 12180

Jacob Fish

Mechanical Engineering Department, Rensselaer Polytechnic Institute, Troy, New York 12180

Pawel Keblinski<sup>a)</sup>

Materials Science and Engineering Department, Rensselaer Polytechnic Institute, Troy, New York 12180

(Received 25 November 2005; accepted 1 February 2006; published online 1 March 2006)

We use a kinetic theory based analysis of heat flow in fluid suspensions of solid nanoparticles (nanofluids) to demonstrate that the hydrodynamics effects associated with Brownian motion have only a minor effect on the thermal conductivity of the nanofluid. This analysis is supported by the results of molecular dynamics simulations of heat flow in a model nanofluid with well-dispersed particles. Our findings are consistent with the predictions of the effective medium theory as well as with recent experimental results on well-dispersed metal nanoparticle suspensions. © 2006 American Institute of Physics. [DOI: 10.1063/1.2179118]

Over the last decade a significant research effort has been committed to exploring the thermal transport properties of colloidal suspensions of nanosized solid particles (nanofluids).<sup>1</sup> In particular, a diverse body of experimental work has demonstrated that the increases in the thermal conductivity with increasing volume fraction of nanoparticles can be significantly larger than predicted by the effective medium theory of a composite material comprised of well-dispersed particles.<sup>2-4</sup>

A number of possible origins for this behavior have been proposed,<sup>5-8</sup> with a consensus yet to emerge.<sup>9</sup> In particular, several authors<sup>6-8</sup> have argued that the large thermal conductivity increases are due to the hydrodynamic effects of Brownian motion of nanoparticles. These authors argued that each Brownian particle generates a long velocity field in the surrounding fluid, akin to that present around a particle moving with a constant velocity, that decays approximately as the inverse of the distance from the particle center. The ability of large volumes of fluid dragged by the nanoparticles to carry substantial amount of heat was credited for large thermal conductivity increases of nanofluids.

In this letter we discuss a kinetic theory based argument suggesting that the Brownian motion contribution to the thermal conductivity of the nanofluid is very small and cannot be responsible for the extraordinary thermal transport properties of nanofluids. We support our argument with the results of molecular dynamics simulations of a model nanofluid. These results are in good agreement with the predictions of the effective medium theory, as well as with the result of recent thermal transport measurements on nanofluids with well-dispersed metal nanoparticles.<sup>10</sup>

In our considerations we will limit ourselves to stationary fluids. To provide an estimate for the contribution of the Brownian motion induced nanoscale fluid flow to thermal conductivity we assume that the entire volume of the fluid diffuses together with the nanoparticles, and that the velocity of the fluid is the same as the velocity of the particles. With

these assumptions, which clearly overestimate the actual magnitude of the fluid velocity field, a well-known kinetic theory formula<sup>11</sup> gives Brownian motion induced contribution to the thermal conductivity,  $\kappa_B$ , as

$$\kappa_B = D_B c_p, \quad (1)$$

where  $c_p$  is the heat capacity of the fluid per unit volume at constant pressure, and  $D_B$  is the diffusivity of the nanoparticles. We note that due to the much higher volume of the fluid at low particle volume fraction, the particles themselves carry much less heat than the fluid moving together with particles. Therefore we neglect the direct contribution of particle Brownian motion to thermal transport.

The thermal conductivity of the base fluid,  $\kappa_F$ , can be also written in the form of Eq. (1) as

$$\kappa_F = D_T c_p, \quad (2)$$

where  $D_T$  is the thermal diffusivity of the fluid defined as  $D_T = \kappa_F / c_p$ .

The ratio of  $\kappa_B$  to  $\kappa_F$  can be evaluated by combining Eqs. (1) and (2),

$$\kappa_B / \kappa_F = D_B / D_T, \quad (3)$$

i.e., the ratio of the Brownian motion contribution to the thermal conductivity to the thermal conductivity of the base fluid is given by the ratio of the nanoparticle diffusivity to the fluid thermal diffusivity.

As a numerical example we consider a water suspension of nanoparticles of radius  $R = 5 \times 10^{-9}$  m at room temperature, at which water has a thermal diffusivity,  $D_T = 1.4 \times 10^{-7}$  m<sup>2</sup>/s and viscosity  $\eta = 10^{-3}$  kg/m s. The Stokes-Einstein formula,  $D_B = k_B T / 6\pi\eta R$ , with the Boltzmann's constant  $k_B = 1.4 \times 10^{-23}$  J/K, gives the nanoparticle diffusivity,  $D_B = 4.5 \times 10^{-11}$  m<sup>2</sup>/s. These lead to the ratio of thermal conductivities  $\kappa_B / \kappa_F = D_B / D_T = 3.2 \times 10^{-4}$ .

This very small ratio of  $\kappa_B / \kappa_F$  (<1%), shows that the Brownian motion induced nanoscale fluid flow has a negligible effect on thermal transport and certainly cannot explain 10% or larger increases of  $\kappa_F$  observed in experiment on nanofluids with very low volume fraction of particles.<sup>2-4</sup>

<sup>a)</sup> Author to whom correspondence should be addressed; electronic mail: keblip@rpi.edu

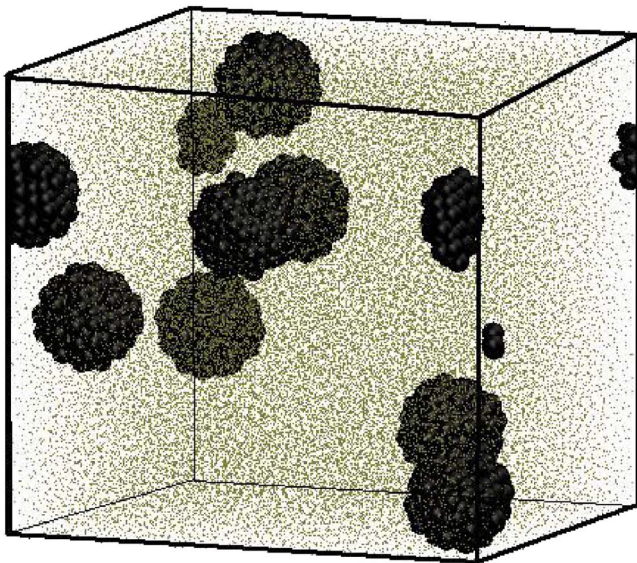


FIG. 1. Snapshot of atomic positions of the nanofluid model structure comprised of 8 crystalline nanoparticles embedded in a liquid.

From the above considerations it is also clear why the Brownian motion is not important for thermal transport. Simply, the heat transport via a conduction mechanism, quantified by the thermal diffusivity, is much faster than the nanoparticle motion, quantified by the particle diffusivity.

To provide further support for our argument, without resorting to simplifying assumptions used in the analysis presented above, we performed molecular dynamics simulations of heat flow in a model nanofluid comprising of crystalline nanoparticles embedded in a fluid.

The interactions between fluid atoms are described by the standard Lennard-Jones (LJ) potential, with pair interaction energy  $U_{LJ}(r)=4\epsilon[(\sigma/r)^{12}-(\sigma/r)^6]$ , where  $\epsilon$  and  $\sigma$  are the units of energy and length, respectively. For computational efficiency we selected a cutoff distance  $R_c=2^{1/6}\sigma$ , which is at the minimum of the LJ potential leading to purely repulsive interactions. The solid particles are formed by carving spheres out of a fcc lattice of atoms. These atoms, in addition to the repulsive LJ interaction, are connected with the nearest neighbors by attractive springs described by a FENE potential<sup>12</sup>  $U_{FENE}=-5.625\epsilon \ln[1-(r/1.5\sigma)^2]$ . There are 296 atoms in each particle, leading to a radius,  $R\approx 4\sigma$ . To mimic solid particles, the masses of atoms forming nanoparticles are three times larger than the mass of the fluid atom, resulting in a particle density about 4.5 times larger than the fluid density. The cross interactions between fluid and solid particles are also described by the LJ potential but with a cutoff of  $1.5\sigma$  leading to attractive forces between fluid and solid particles. For this cutoff, the LJ potential is modified such that both energy and force are equal to zero at the cutoff distance.<sup>13</sup> Three solid-fluid interaction strengths were used,  $\epsilon_{SF}=0.25\epsilon$ ,  $1.25\epsilon$ , and  $2.25\epsilon$ . These three choices lead to a range of wetting properties, and are referred to throughout as nonwetting, weakly-wetting, and wetting particle cases, respectively.

In our model nanofluid total of eight particles are suspended in 50 000 fluid atoms (see Fig. 1) at a pressure corresponding to that characterizing pure fluid with density of 0.81 particles per  $\sigma^3$  thick bins. The edge length of the corresponding periodic cubic simulation box is about  $40\sigma$ . This

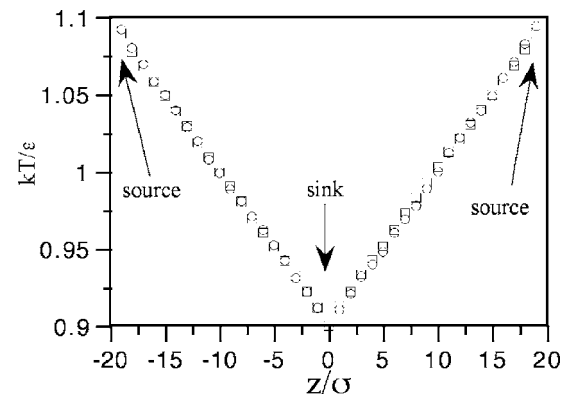


FIG. 2. Temperature profiles obtained from the heat source-sink simulations for pure fluid (circles) and wetting particle nanofluid (squares). The slope of the temperature profile allows the thermal conductivity to be determined. The arrows indicate positions of the heat source and sink.

choice leads to a nanofluid with a particle volume fraction of about 3.3%. Before the thermal transport simulations, each structure was equilibrated for 200 000 MD steps at constant volume and temperature,  $T=1.0\epsilon/k_B$ . A MD time step of  $0.005\tau_{MD}$  ( $\tau_{MD}=\sqrt{\epsilon/m\sigma^2}$ , where  $m$  is the fluid atom mass) and the Verlet integration algorithm are used in all simulations.<sup>13</sup>

To determine the thermal conductivity, we use the so-called direct method where a planar heat source and sink are applied with the overall thermostat turned off. The planar sink and source regions are both  $1\sigma$  wide and are located at the center and at the edge of the periodic simulation box. Atomic velocities were scaled up (down) in the heat source (sink) regions so that heat was added at a constant rate of  $dQ/dt=200\epsilon/\tau_{MD}$ , to the source and removed at the same rate from the sink. We determined the temperature profile along the  $z$  direction by calculating the total kinetic energy of the atoms (both solid and fluid) in  $1\sigma$  thick bins.

Upon the application of the heat source and sink, a steady state temperature profile is established in the first  $\sim 100$  000 MD steps, after which we collect the average temperature profile data over 200 000 MD steps. Examples of such temperature profiles are shown in Fig. 2. The profiles allow us to determine the thermal conductivity of the nanofluid,  $\kappa_{NF}$ , using Fourier's Law,  $j_Q=-\kappa\partial T/\partial z$ , where  $j_Q=(dQ/dt)/2A$  is the heat flux, with  $A$  being the cross-sectional area (the factor of 2 accounts for heat flow in both positive and negative  $z$  directions in periodic systems). We note that we did not observe any persistent clustering during our simulations, and the particles, while moving randomly, maintained good dispersion in the fluid throughout the simulation run.

Our key thermal transport results are presented in Table I, showing the thermal conductivity of three nanofluids in the reduced LJ units,  $k_B/\sigma\sqrt{\epsilon/m\sigma^2}$ , where  $k_B$  is the Boltzmann constant. As a reference condition, we also simulated the pure fluid for which we obtained,  $\kappa_F=6.33$ . In all cases we observe only minor differences of thermal conductivity compared to that of the pure fluid. The thermal conductivity of nanofluids with nonwetting and weakly wetting particles is slightly lower than that of the nanofluid with wetting particles. Even with wetting particles the thermal conductivity increase is rather small and does not correspond to spectacular increases observed in experiment.<sup>2-4</sup>

TABLE I. Thermal transport data of the nanofluids with no-wetting, weakly-wetting, and wetting particle. Interfacial resistance in units of the equivalent fluid thickness,  $h$ , nanofluid thermal conductivity,  $\kappa_{\text{NF}}$ , in reduced LJ units. Ratios  $\kappa_{\text{NF}}/\kappa_F$  obtained from MD simulations with  $\kappa_F=6.33$  are compared against the predictions of the effective medium theory [Eq. (4)].

$\epsilon_{\text{SF}}$ interaction strength	$h$ equivalent matrix thickness	$\kappa_{\text{NF}}$ MD results	$\frac{\kappa_{\text{NF}}}{\kappa_F}$ MD results	$\frac{\kappa_{\text{NF}}}{\kappa_F}$ effective medium theory
0.25	$5.2 \pm 0.5$	$6.39 \pm 0.05$	$1.0095 \pm 0.01$	$0.992 \pm 0.01$
1.25	$3.8 \pm 0.3$	$6.39 \pm 0.04$	$1.010 \pm 0.01$	$1.002 \pm 0.007$
2.25	$1.8 \pm 0.2$	$6.48 \pm 0.05$	$1.025 \pm 0.01$	$1.028 \pm 0.005$

The differences in thermal conductivity of the three model nanofluids originate from the differences in the interfacial thermal resistance of the solid-fluid interfaces.<sup>14</sup> We evaluate this resistance by MD simulations in which a single particle is heated at a constant rate and the heat is removed from a spherical fluid shell away from the particle. The resulting radial temperature profiles in the fluid (not shown) were essentially the same, and follow the well-known solution of the steady state heat flow problem with spherical symmetry,  $T=B+A/r$ , where  $B$  and  $A$  are constants related to the magnitude of generated heat and fluid thermal conductivity. However, at the solid fluid interface we observed a temperature jump associated with interfacial thermal resistance, which was particularly large for the nonwetting particle case.<sup>15</sup> The so-called equivalent matrix thickness  $h$ , over which the temperature drop is the same as at the interface in the planar heat flow geometry is listed in Table I.

Knowledge of the interfacial thermal resistance, particle size, and volume fraction allows estimation of the nanofluid conductivity according to the effective medium (EM) theory. We used EM theory in the limit of particles being much more conductive than fluid; from the temperature profiles obtained for solid particles alone we estimated that particles are at least ten times more conductive than fluid. The EM theory at low volume fractions of well-dispersed thermally conductive nanoparticles, predicts<sup>14</sup>

$$\frac{\kappa_{\text{NF}}}{\kappa_F} = 1 + 3f \frac{\gamma - 1}{\gamma + 2}, \quad (4)$$

where  $f$  is the particle volume fraction, and  $\gamma$  is the ratio of the particle radius to the equivalent matrix thickness  $h$ . According to Eq. (4) with no interfacial resistance ( $\gamma \rightarrow \infty$ ) the

ratio  $\kappa_{\text{NF}}/\kappa_F$  has a maximum value of  $1+3f$ . When the particle radius becomes equal to the equivalent matrix thickness ( $\gamma=1$ ) there is no thermal conductivity enhancement at all, while for larger interfacial resistance ( $\gamma < 1$ ) the addition of particles decreases the thermal conductivity of the fluid, as the particles act as insulating holes. The results of our simulations, within the error bars, are in very good agreement with predictions of the EM theory, as shown by the data in Table I.

In summary, we have presented a kinetic theory argument and the results of molecular dynamics simulations, both leading to a conclusion that the thermal conductivity of a nanofluid with well dispersed nanoparticles is well described by the effective medium theory and does not show any significant enhancements due to effects associated with Brownian motion induced hydrodynamic effects. Our conclusions are in agreement with results of recent experiments on thermal conductivity of suspension of well-dispersed metal nanoparticles,<sup>10</sup> and suggest that other effects, such as particle clustering, are responsible for large thermal conductivity increases observed in “experiment.”

This work was supported by DOE Grant No. DE-FG02-04ER46104.

<sup>1</sup>For a recent review, see J. A. Eastman, S. R. Phillpot, S. U.-S. Choi, and P. Koblinski, *Annu. Rev. Mater. Res.* **34**, 219 (2004).

<sup>2</sup>J. A. Eastman, S. U. S. Choi, S. Li, W. Yu, and L. J. Thompson, *Appl. Phys. Lett.* **78**, 718 (2001).

<sup>3</sup>H. E. Patel, S. K. Das, T. Sundararajan, A. S. Nair, B. George, and T. Pradeep, *Appl. Phys. Lett.* **83**, 2931 (2003).

<sup>4</sup>T.-K. Hong, H.-S. Yang, and C. J. Choi, *J. Appl. Phys.* **97**, 64311 (2005).

<sup>5</sup>P. Koblinski, S. R. Phillpot, S. U. S. Choi, and J. A. Eastman, *Int. J. Heat Mass Transfer* **45**, 855 (2002).

<sup>6</sup>S. P. Jang and S. U. S. Choi, *Appl. Phys. Lett.* **84**, 4316 (2004).

<sup>7</sup>R. Prasher, P. Bhattacharya, and P. E. Phelan, *Phys. Rev. Lett.* **94**, 025901 (2005).

<sup>8</sup>J. Koo and C. Kleinstreuer, *J. Nanopart. Res.* **6**, 577 (2004).

<sup>9</sup>P. Koblinski, J. A. Eastman, and D. G. Cahill, *Mater. Today* **8**, 36 (2005).

<sup>10</sup>S. A. Putnam, D. G. Cahill, P. V. Braun, Z. Ge, and R. G. Shimmin (submitted). Available at: <http://users.mrl.uiuc.edu/cahill/preprints.html>

<sup>11</sup>See, for example, F. Reif, *Fundamentals of Statistical and Thermal Physics* (McGraw-Hill, New York, 1965), pp. 478–482.

<sup>12</sup>G. S. Grest and K. Kremer, *J. Chem. Phys.* **92**, 5057 (1990), and references therein.

<sup>13</sup>M. P. Allen and D. J. Tildesley, *Computer Simulation of Liquids* (Oxford University Press, Oxford, 1992).

<sup>14</sup>S. A. Putnam, D. G. Cahill, B. S. Ash, and L. S. Schadler, *J. Appl. Phys.* **94**, 6785 (2003).

<sup>15</sup>L. Xue, P. Koblinski, S. R. Phillpot, S. U.-S. Choi, and J. A. Eastman, *J. Chem. Phys.* **118**, 337 (2003).